Cellulose (2023) 30:775–787
https://doi.org/10.1007/s10570-022-04961-4

ORIGINAL RESEARCH

Aqueous bifunctionalization of cellulose nanocrystals through amino and alkyl silylation: functionalization, characterization, and performance of nanocrystals in quartz microflotation

Feliciana Ludovici · Robert Hartmann · Henrikki Liimatainen

Received: 11 July 2022 / Accepted: 18 November 2022 / Published online: 27 November 2022

Abstract Surface modifications of cellulose nanomaterials can be used to tailor their surface charge and hydrophilicity-hydrophobicity characteristics. Additionally, it can facilitate the selective interaction of nanocelluloses with other solid particles to further expand their applicability in different fields. For instance, cellulose nanocrystals (CNC) with amphiphilic features are potential green alternatives in mineral processing such as particle flotation. In the present study, aqueous, one- and two-step silylation of CNCs with amino and alkyl silanes was considered to create a novel bifunctionalized CNCs that contained both positively charged amino silane moieties and hydrophobic alkyl chains. Especially, the effects of reaction conditions and different reaction routes on the silylation were investigated, and the electric surface potential and hydrophobicity of CNCs were determined. The bifunctionalization conducted by the simultaneous addition of an amino silane and alkyl silane led to a high reaction efficiency, and the grafting amount was notably higher than that obtained with the sequential reactions with individual reagents. After the functionalization, the hydrophobicity of the CNCs was strongly altered, leading to water contact angles of up to 135° on CNC films. However, the silylation with amino silanes slightly affected the ζ-potential of the functionalized CNCs. Due to the relatively low ζ-potential, the interaction and orthokinetic attachment of CNCs onto quartz surfaces were insufficient, resulting in a limited flotation recovery in microflotation using a Hallimond tube.

Keywords Cellulose nanoparticles · Deep eutectic solvent · Nanocellulose · Silane · Wettability · Quartz microflotation

Supplementary Information The online version contains supplementary material available at https://doi.org/10.1007/s10570-022-04961-4.

F. Ludovici · H. Liimatainen (✉)
Fiber and Particle Engineering Research Unit, University of Oulu, P. O. Box 4300, 90014 Oulu, Finland
e-mail: henrikki.liimatainen@oulu.fi

R. Hartmann
Department of Chemical and Metallurgical Engineering, School of Chemical Engineering, Aalto University, P.O. Box 12200, 00076 Espoo, Finland

R. Hartmann
Fraunhofer Center for Chemical-Biotechnological Processes, 06237 Leuna, Germany

Introduction

Cellulose is an amenable substrate to different functionalization reactions and a promising candidate for creating diversity in advanced, green, renewable, and biodegradable materials. Notably, the aqueous silylation reactions have been thoroughly investigated as straightforward and eco-friendly approaches to incorporate various functional groups (alkyl-, vinyl-, thiol-, azido-, amino- groups, among

others) on cellulose and promote cellulose cross-linking (Abdelmouleh et al. 2002) (Abdelmouleh et al. 2004) (Andresen et al. 2006) (Daniels and Francis 1998) (Indarti et al. 2019) (Khanjanzadeh et al. 2018) (Goussé et al. 2004) (Geng et al. 2017) (Jarrah et al. 2018) (Yu et al. 2019) (Zhang et al. 2015) (Zhang et al. 2014) (Beaumont et al. 2018). Silylation reactions represent a feasible way to functionalize cellulose substrates, enabling their use in different applications, such as antibacterial and antimicrobial materials or as flocculants in the mining industries (Coelho Braga de Carvalho et al., 2021) (Fernandes et al. 2013) (Saini et al. 2017). Several articles have described the reaction mechanism between cellulose and silane-based reagents (Salon et al. 2007) (Brochier Salon and Belgacem 2010) (Rafieian et al. 2019) (Osterholtz and Pohl 1992) (Hettegger et al. 2016). The mechanism comprises three main steps, starting from the hydrolysis of the pristine silane compounds to obtain silane derivatives. Then, the adsorption of the silane derivatives on the cellulose surface occurs through hydrogen bonding between the silane and hydroxyl functional groups of the cellulose surface. Finally, chemical condensation and formation of relatively stable Si–O-cellulose bonds occurs, as shown in Fig. 1. During the chemical condensation, thermal activation plays an important role, leading to siloxane bridges. In consequence, the three alkoxy groups in the pristine silane compounds may not solely undergo a condensation reaction with the hydroxyl groups of the cellulose substrate, but may also self-condense, leading to the formation of dimeric or oligomeric structures, thus they cannot be adsorbed on the cellulose surface (Daniels and Francis 1998).

The silylation modifications are conducted in aqueous media, so the hydrolysis and thus the condensation and self-condensation are strongly affected by reaction conditions. The effect of pH on the hydrolysis kinetics and the grafting of alkoxysilane compounds has been intensively revealed (Salon et al. 2007) (Brochier Salon et al. 2005) (Brochier Salon and Belgacem 2010). The hydrolysis rate of various silane reagents has been reported to be very low under neutral conditions, except for aminosilane (3-aminopropyl-triethoxysilane, APTES), which, also under acidic conditions, displayed the fastest reaction rate and underwent the hydrolysis and condensation reactions (Brochier Salon et al. 2008). However, the hydrolysis reaction of triethoxy-n-octylsilane (OTS)

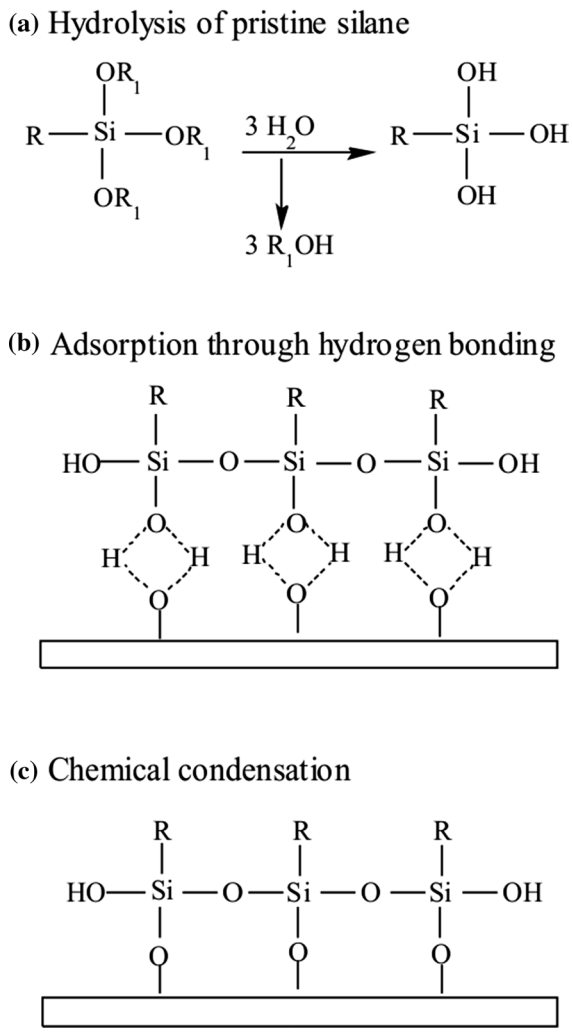

Fig. 1 The reaction mechanism between cellulose and silane-based reagents

was extremely slow under acidic conditions but even slower under neutral or alkaline conditions. In alkaline conditions, OTS hydrolysis was accelerated by triethylamine (TEA) catalyst; a ten-fold excess of TEA was required to accelerate the reaction (Brochier Salon et al. 2008) (Brochier Salon and Belgacem 2011). Moreover, the effects of temperature, pH, organic solvents, concentration and amount of water, catalyst, and silane structure on the reaction rates and mechanisms have been investigated (Osterholtz and Pohl 1992).

The present study investigates the aqueous surface modification of CNCs with amino silane or alkyl silanes with propyl, hexyl, or octyl chains,

respectively, or a mixture of both silanes to obtain bifunctionalized CNCs. Especially, it was aimed at obtaining a novel type of bifunctionalized, mixed CNCs that contain both positively charged surface moieties and alkyl chains to enhance the hydrophobic character of the nanoparticles. Previous studies indicated that the silylation reactions effectively increase the hydrophobic properties of the functionalized cellulose samples. The role of reaction conditions and different reaction routes were revealed, and the electric surface potential and hydrophobicity of CNCs were determined. Finally, the performance of the functionalized CNCs as flotation agents for quartz particles in Hallimond tube microflotation was elucidated.

Experimental

Materials

For the functionalization reactions, two different cellulose nanocrystal (CNCs) samples were used as starting materials. A commercial CNC sample (BGC) was purchased (Blue Goose Biorefineries, Canada) and used as received, without any further purification. The BGC production process was based on the oxidation of acetate-grade dissolving pulp (*Western hemlock*) and did not involve acid hydrolysis. Secondly, a deep eutectic solvent system (DES) was used to obtain CNCs from a dry sheet of industrial bleached birch (*Betula verrucosa*) kraft pulp, which was purchased from UPM (Finland). A mixture of oxalic acid dihydrate (Sigma-Aldrich, India) and choline chloride (TCI, Japan) was used to produce a deep eutectic solvent system (Sirviö et al. 2016).

The silylation reagents, i.e., 3-aminopropyltriethoxysilane (APTES, 98%) and n-propyltriethoxysilane (PTS, 97%), were purchased from Sigma-Aldrich (USA), while hexyltriethoxysilane (HTS, 97%) and triethoxy-n-octylsilane (OTS 97%), were obtained from VWR TCl Europe (Belgium). Ethanol (96% v/v) solution was supplied by VWR, BDH Chemicals (France). For pH adjustment, diluted NaOH and HCl solutions (Oy FF-Chemicals Ab, Finland) were used. All the reagents were used as received without any further purification. Deionized water (18.2 MΩcm) was used throughout the experiments.

The quartz sample, mainly consisting of SiO_2 (purity ~ 98 wt. % SiO_2), as shown in a previous study (Coelho Braga de Carvalho et al., 2021), was obtained from Schlingmeier Quarzsand GmbH & Co. KG (Germany). The mineral was received with a $d_{80} < 100$ µm, and no further grinding was applied before microflotation experiments. The initial quartz sample was placed on sieves with a 100 and 90 µm mesh size to obtain a coarse sample and rinsed with a copious amount of deionized water to remove fines. The obtained sample was dried in an oven overnight at 50℃. The final particle size distribution was then analyzed with a Beckman Coulter LS 13 320 (USA) under wet conditions, and the results are shown in Fig. S1.

Methods

Production of cellulose nanocrystals using a deep eutectic solvent

For hydrolysis of kraft cellulose pulp and production of CNCs, deep eutectic solvent (DES) of choline chloride and oxalic acid dihydrate was used at a molar ratio of 1:1, using a method described in a previous work (Sirviö et al. 2016). The constituents were mixed and heated to 100 °C for 30 min, after which 5 g of dried pulp was added into 500 g of DES solution, and subsequently mixed at 100 °C for 6 h. After mixing, the dispersion was removed from the heating source (oil bath), and 100 mL of deionized water was added. The pre-treated pulp dispersion was vacuum-filtered and washed with deionized water until a neutral pH value was reached.

Using a dilute NaOH solution, the pH value of the aqueous DES-treated cellulose dispersion was adjusted to 7. Finally, the dispersion was mechanically treated using a microfluidizer (Microfluidics M/110Eh/ 30, USA) to obtain individualized cellulose nanocrystals. Three passes through 400 and 200 µm chambers at a pressure of 1000 bar, and then three passes through 200 and 100 µm chambers at a pressure of 1500 bar were applied.

Silylation of cellulose nanocrystals

An aqueous silylation reaction was used to obtain three different functionalized cellulose nanocrystal

samples, i.e., CNCs containing an amino silane group (termed as BGC-/DES-ami), CNCs containing alkyl silane chains (termed as BGC-propyl, -hexyl, or -octyl), and mixed BGC containing both amino and alkyl silane chains (termed as BGC-mix). The synthetic routes to obtain silylated cellulose nanocrystals with different grafting contents and functionalities, and the used reaction conditions are presented in Fig. 2 and Tables 1, 2 3.

Using different cellulose-reagent mass ratios, pH values, CNC solid contents (wt%), and heating times, the pristine CNCs (BGC or DES) reacted with a chosen silane reagent (APTES, PTS, HTS, or OTS). Before the silylation reaction, the pH value of the CNC suspension was adjusted to either 4 using a 1 M HCl solution or to 10 using a 1 M NaOH solution. Meanwhile, by dissolving the desired silane reagent in ethanol while mixing with a magnetic stirrer for 10 min, a fresh silane solution (10% w/w) was prepared. Then, the silane solution was added dropwise to the aqueous CNC suspension using a micropipette, while constantly stirring at room temperature for 2 h. Finally, the CNC suspension was heated at 80℃ for a pre-defined time.

For the preparation of BGC-mix samples, three different reaction pathways were investigated. First, both the amino and alkyl-containing silylation reagents (propyl or hexyl groups) were simultaneously added to the BGC pulp (BGC-mix 9 and BGC-mix 12, respectively). Then, a two-step sequential reaction was conducted, in which the amino-containing reagent was added first, followed by adding the propyl chain-containing reagent (BGC-mix 10). Finally, a second two-step sequential reaction was conducted, in which the propyl chain-containing reagent was added first, followed by adding amino-containing reagent (BGC-mix 11). After the reactions, all the functionalized CNC samples were washed with deionized water and EtOH (1:1 H_2O/EtOH), and centrifuged (5 min, 6000 rpm, 20℃, using Beckman Coulter Avanti J-26 XP; USA). Finally, the sediment was collected while the clear supernatant was disposed. The washing procedure was repeated three times.

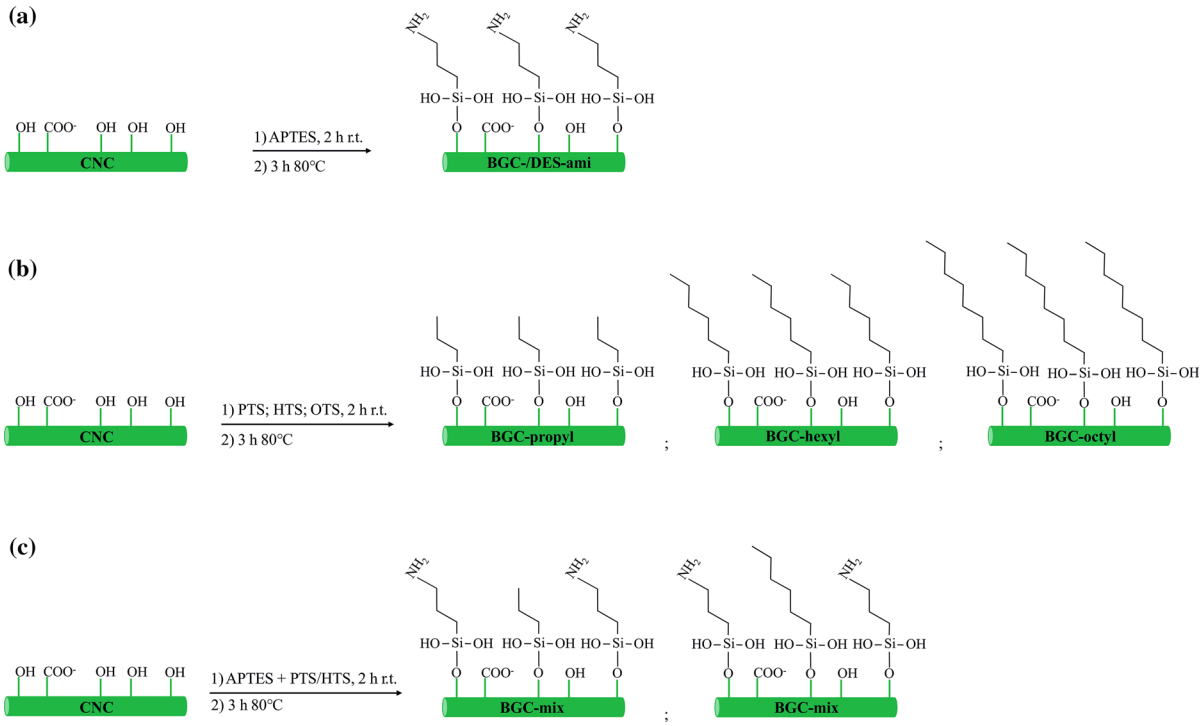

Fig. 2 Functionalization of CNCs in two steps: (1) stirring 2 h at room temperature, (2) stirring 3 h at 80 ℃, grafted with **a** amino silane (BGC-ami/DES-ami), **b** alkyl silane (BGC-propyl, -hexyl, or -octyl), or **c** amino and alkyl (propyl or hexyl) silanes (BGC-mix) via aqueous silylation

Table 1 Functionalization conditions for cellulose nanocrystals (BGC/DES) grafted with an amino silane

	DES-ami 1	DES-ami 2	DES-ami 3	DES-ami 4	DES-ami 5	BGC-ami 1	BGC-ami 2	BGC-ami 3	BGC-ami 4	BGC-ami 5	BGC-ami 6	BGC-ami 7	BGC-ami 8
Mass ratio[1]	1:0.5	1:0.5	1:0.5	1:1	1:1	1:1	1:1	1:1	1:1	1:1	1:1	1:0.5	1:0.1
pH	4	4	4	4	10	4	4	10	10	10	10	10	10
CNC (wt%)	0.5	0.5	0.5	1	1	0.5	1	0.5	1	1	1	1	1
Heating time (h)	1	2	3	3	3	3	3	3	3	1	2	3	3

[1]Cellulose/silylation agent mass ratio

Table 2 Functionalization conditions for cellulose nanocrystals (BGC) grafted with alkyl silane

	BGC-propyl	BGC-hexyl	BGC-octyl
Mass ratio	1:1	1:1	1:1
pH	4	4	4
CNC (wt%)	1	1	1
Heating time (h)	3	3	3

X-ray photoelectron spectroscopy analysis and grafting amount

For pristine and silylated CNCs films, carbon, oxygen, nitrogen, and silicon contents were analyzed. The films were prepared by diluting the pristine and silylated CNCs samples in 40 mL deionized water to a final consistency of 0.5% w/w and then dried overnight at 50℃. The X-ray photoelectron spectra of the silylated CNC films were measured using an X-ray photoelectron spectrometer Quantum 2000, (Physical Electroncs Inc., US) with a monochromatic Al-Kα (1486.6 eV) source. The grafting amount (GA) of amino silane groups ($mmol_{reagent}/g_{CNC}$) was calculated based on the nitrogen content of the CNCs-ami and BGCs-mix, while the GA of alkyl silane groups was determined from silicon contents using the following equations:

$$GA = \frac{N\% * 1000}{AW_N} \tag{1}$$

$$GA = \frac{Si\% * 1000}{AW_{Si}} \tag{2}$$

where, *N*% and Si% are nitrogen and silicon content, and AW refers to the atomic weight of either nitrogen (*N*) or silicon (Si).

Transmission electron microscopy

The morphology of the pristine DES CNC samples was studied using transmission electron microscopy, (JEM-2200FS, JEOL Ltd., Tokyo, Japan). A small droplet of 0.1% poly-L-lysine suspension was added to the top of a carbon-coated copper grid, to obtain a cationic grid surface. The DES CNC was firstly diluted to 0.1% w/w with deionized water. Then, a

Table 3 Functionalization conditions for cellulose nanocrystals (BGC) containing both amino and alkyl silane moieties: (1) propyl chain and (2) hexyl-chain

	[1]BGC-mix 9	[1]BGC-mix 10	[1]BGC-mix 11	[2]BGC-mix 12
Mass ratio	1:0.5:0.5	1:0.5:0.5	1:0.5:0.5	1:0.5:0.5
pH	10	10	10	10
CNC (wt%)	1	1	1	1
Heating time (h)	3	3	3	3

small droplet was placed on the grid. Finally, a 2% uranyl acetate solution was dropped to negatively stain the sample. The excess was removed by dipping the grid into a beaker containing deionized water. The sample was dried overnight at room temperature and analyzed using an acceleration voltage of 200 kV under standard conditions. Images were captured using the EM-Menu software, where the ImageJ software was used to measure the length and width of the individual cellulose nanocrystals.

Surface (ζ-) potential

The electric surface (ζ-) potential of aqueous suspensions of pristine and silylated cellulose nanocrystals (both DES and BGC CNC samples) was measured at pH of 3, 6, and 9 by adjusting the pH value using either a dilute HCl or NaOH solution. The CNC suspensions were diluted by adding 100 µL of 0.1% w/w aqueous CNC sample to 10 mL of a 10 mM NaCl background solution. The measurements were conducted as a function of the pH value using a Malvern ZetaSizer NanoZS (Malvern Panalytical, UK) at room temperature with six repetitions for each sample.

Contact angle measurement

The static and dynamic contact angles of a sessile drop on silylated cellulose nanocrystal films were measured using an OCA 50 (DataPhysics, Germany). For preparing cellulose films, the CNC samples were diluted in 40 mL with deionized water to a final consistency of 0.5% w/w and then dried in an oven at 50 °C to obtain self-standing films. For the contact angle measurements, a drop (8 µL) of deionized water was placed on a cellulose film surface, and the static contact angle was measured. Subsequently, dynamic, i.e., advancing and receding contact angles (ARCA), were detected via the needle-in-drop method. The needle was immersed in the droplet, and an additional 8 µL of deionized water was sequentially added and retracted from the droplet until 5 repetitions were performed. The ARCAs were instantly recorded with a frame rate of 2 images per second. For each sample, five droplets were placed in different locations on the cellulose film and analyzed with SCA20 software using the ellipse-fitting model, which can measure the contact angle of a non-asymmetric drop.

Quartz microflotation tests

An in-house build Hallimond tube (200 mL) was used for quartz microflotation experiments. Before the measurement, 1.0 g of the quartz sample was added into 100 mL of a 10 mM NaCl background solution with a pH value of 3. The slurry was mixed with a magnetic stirrer for 5 min, followed by adding a predefined quantity of CNC suspension to obtain a concentration of 5 mg/L in the slurry. After the second conditioning for 5 min, the slurry was transferred into the Hallimond tube and adjusted to the desired water level with the background solution. For the flotation, nitrogen gas was used at a flow rate of 25 mL/min using a flotation time of 5 min. The collected quartz from over- and under-flow was separately filtered, dried, and weighed to determine recoveries.

Results and discussion

Functionalization of cellulose nanocrystals through aqueous silylation

A commercial CNC sample (BGC) and CNCs obtained from a DES treatment were used as substrates for the functionalization reactions. These CNC specimens differed especially in terms of their surface charge density, as the DES treatment results in partial esterification of cellulose by oxalic acid (DS of 0.2–0.3 mmol/g) (Sirviö et al. 2016), while the content of anionic functional groups in BGC was very low (< 0.1 mmol/g). The zeta potential of the CNCs is

presented in Fig. S2. According to TEM analysis, the BGC consisted of rod-like cellulose nanocrystals possessing an average width of 3–8 nm and a length of 50–350 nm (Laitinen et al. 2017). A combined treatment with DES of choline chloride and oxalic acid and microfluidizer led to the individualized CNCs, having an average width of 4 nm and a length of 150 nm, as visualized via TEM images in Fig. S3.

Aqueous silylation of CNCs was conducted using three different modification routes based on reaction with amino silane (APTES) or alkyl silanes with propyl, hexyl, or octyl chains (PTS, HTS, or OTS, respectively), or a mixture of both silanes to obtain bifunctionalized CNCs (Fig. 2). The influences of pH on the hydrolysis of the pristine silane compounds and reaction efficiency were elucidated, and the role of the reaction time in the silane condensation was revealed at 80℃. The GA of the CNCs was determined via X-ray photoelectron spectroscopy using Eqs. 1 and 2. The elemental contents of carbon, nitrogen, oxygen, and silicon of pristine and modified CNCs are summarized in Table S1.

Aqueous silylation of CNCs with amino silane

Initially, the APTES grafting on the cellulose substrate (DES CNCs) was evaluated as a function of the condensation (heating) time (1–3 h) with DES CNCs, as shown in Fig. 3. The other reaction parameters, namely cellulose-APTES mass ratio (1:0.5), pH (4), and initial CNC consistency (0.5% w/w) were kept constant. The final GA was not strongly affected by the increase in the condensation time, and the low pH resulted in a low grafting amount, (< 0.3 mmol/g), despite the prolonged heating time. Previous studies have indicated that acidic media enhance the hydrolysis of the silanes bearing an amine functionality, and promote self-condensation reaction, leading to the formation of three-dimensional silane networks (Brochier Salon and Belgacem 2010) (Brochier Salon et al. 2008). The obtained results (Fig. 3) corroborate these previous findings, and the low GA is presumably caused by the self-condensation of amino silanes instead of the chemical grafting onto the cellulose surfaces.

Subsequently, the role of reaction medium pH and initial CNC consistency in the silylation of CNCs, both BGC and DES, was further revealed (Fig. 4). These experiments were conducted both in acidic and alkaline conditions (pH values of 4 and 10, respectively) using CNC contents of 0.5 and 1.0%. The reaction efficiency was notably affected by the solution pH, and the reactions conducted in the alkaline conditions resulted in clearly higher GA values (> 1.3 mmol/g) both with BGC and DES CNCs. Alkaline conditions, indeed, seem to favor the chemical

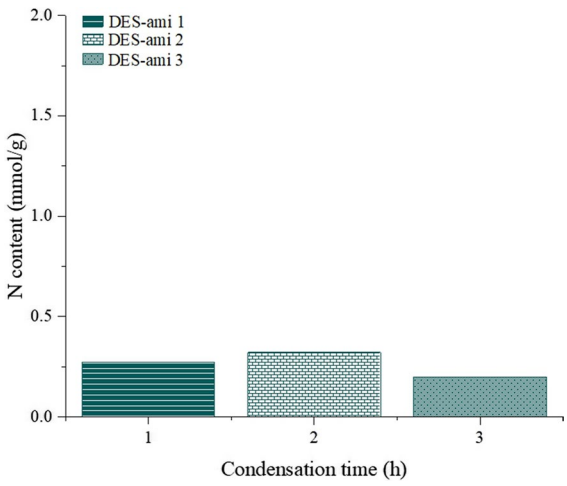

Fig. 3 Grafting amount of silylated DES cellulose nanocrystals (CNCs) grafted with amino silane at a pH of 4 as a function of condensation time (CNC consistency of 0.5% w/w and cellulose-silylation reagent mass ratio of 1:0.5)

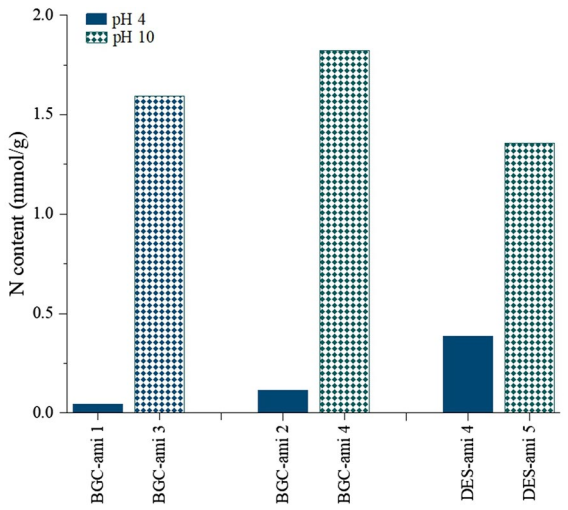

Fig. 4 Grafting amount of silylated cellulose nanocrystals (CNCs) (BGC/DES) grafted with amino silane as a function of pH value (CNC consistency of 0.5% and 1.0% and cellulose-APTES mass ratio of 1:1)

grafting of the hydrolyzed silanes onto the cellulose surfaces instead of the self-condensation reactions. A 37 times higher GA was obtained at pH 10 (BGC-ami 3) compared to that of pH 4 (BGC-ami 1) with an initial BGC CNC consistency of 0.5%; however, a 16 times higher GA was found at an alkaline pH of 10 with an initial CNC consistency of 1% (BGC-ami 4 vs. BGC-ami 2). A similar trend was also observed with DES CNCs, alkaline conditions remarkably facilitated the silylation reaction, resulting in a 3.5 times higher GA compared to that of acidic pH (DES-ami 5 vs. DES-ami 4). However, the GA level was slightly lower with the DES CNCs than that with BGC CNCs (~ 1.4 mmol/g vs. > 1.5 mmol/g). Additionally, the initial CNC consistency had only a minor effect on the final GA, indicating that the increased probability for silane groups to react with the cellulose surface in the reaction suspension had only a minor influence on the silylation reaction.

The influence of condensation time (1–3 h) on silylation with amino silane at alkaline conditions was elucidated in more detail with BGC CNC, which possessed the highest GA (BGC-ami 4). The other reaction parameters, namely cellulose-APTES mass ratio (1:1), pH (10), and CNC initial consistency (1% w/w) were kept constant (Fig. 5). Figure 5 demonstrates that the longer heating time of 3 h promoted the silylation, and the GA increased from ~ 1 to ~ 1.75 mmol/g. Previously, heat treatment has been corroborated to induce the condensation reaction and a final chemical grafting of the hydrolyzed silane (APTES) onto the cellulose surface (Abdelmouleh et al. 2002) (Abdelmouleh et al. 2004) (Khanjanzadeh et al. 2018) (Indarti et al. 2019). Recent results also indicated that the temperature of 80℃ enables a chemical grafting onto the cellulose surface without degrading the cellulose (Indarti et al. 2020).

The effect of the cellulose-reagent ratio on silylation was investigated using APTES mass ratios of 1:0.1, 1:0.5, and 1:1 (BGC-ami 8, BGC-ami 7, and BGC-ami 4, respectively), while keeping the other parameters, i.e., the pH (10), heating time (3 h) and initial CNC consistency (1% w/w) constant. The reaction efficiency strongly correlated with the amount of used silylation reagent. When the ratio increased from 1:0.1 to 1:1, the GA increased from ~ 0.6 to ~ 1.75 mmol/g (Fig. 6).

Aqueous silylation of CNCs with alkyl silanes

Secondly, the functionalization of BGC CNCs with alkyl silanes possessing variable chain lengths (propyl, hexyl, and octyl) was explored. Contrary to grafting with amino silanes, the reactions were performed at a pH of 4, only using a CNC consistency of 1%, condensation time of 3 h, and cellulose-silane reagent mass ratio of 1:1. As shown in Fig. 7, the hexyl silane displayed the highest reactivity, resulting in

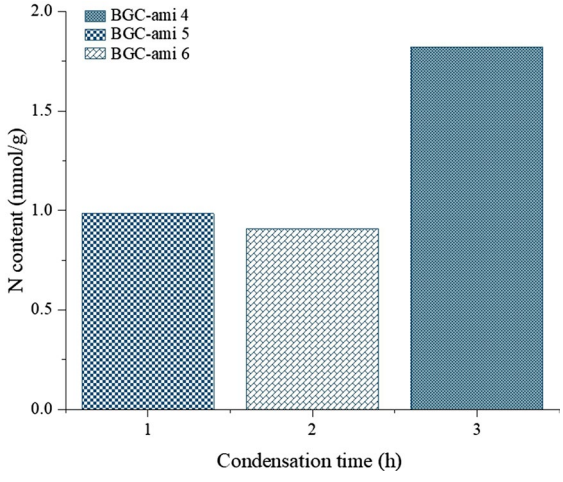

Fig. 5 Grafting amount of silylated BGC cellulose nanocrystals (CNCs) grafted with amino silane at a pH of 10 as a function of condensation time (CNC consistency of 1% and cellulose-APTES mass ratio of 1:1)

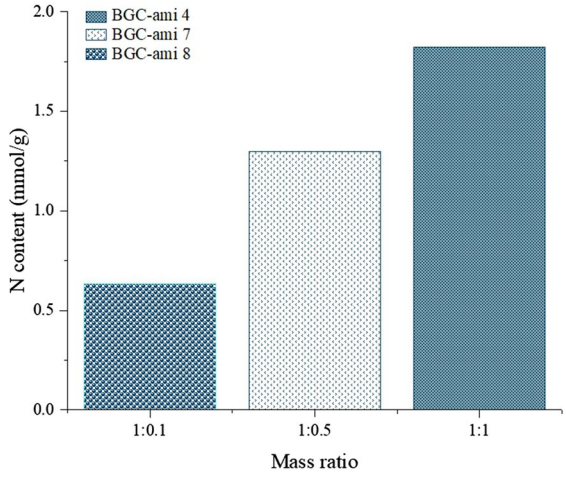

Fig. 6 Grafting amount of silylated BGC cellulose nanocrystals (CNCs) grafted with amino silane at a pH of 10 as a function of cellulose-APTES mass ratio (CNC consistency of 1%)

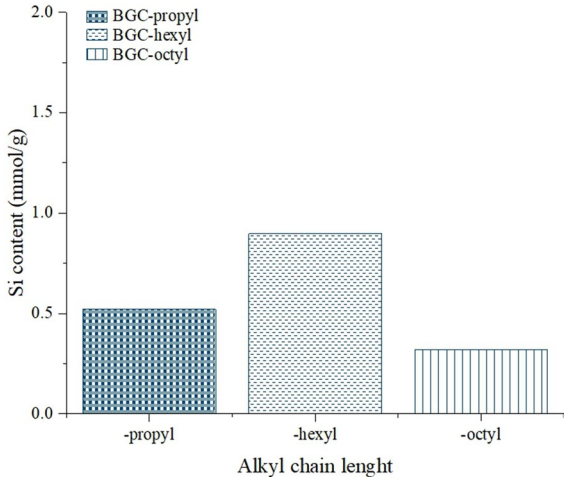

Fig. 7 Grafting amount of silylated BGC cellulose nanocrystals (CNCs) grafted with alkyl silanes having variable chain lengths

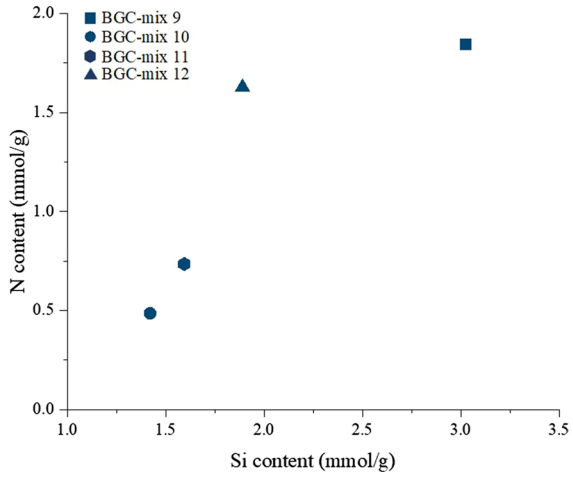

Fig. 8 Grafting amount of bifunctionalized cellulose nanocrystals (CNCs) grafted with amino and alkyl silanes (CNC consistency of 1% and cellulose-silanes mass ratio of 1:0.5:0.5)

GA of 0.897 mmol/g, followed by propyl and octyl silanes (0.52 and 0.32 mmol/g, respectively). Previously, the reaction kinetics associated with triethoxy-n-octylsilane (OTS) at a pH of 4 was noticed to be slower compared to other silane reagents, but it was still much faster than its hydrolysis in neutral and basic conditions (Brochier Salon et al. 2008) (Bel-Hassen et al. 2008) (Brochier Salon and Belgacem 2011). The maximum silane content with OTS was reached after 20 h of reaction time. The hydrolyzed silanes showed high stability toward self-condensation, favored under alkaline conditions. The slow hydrolysis response indeed supports the low obtained GA (0.32 mmol/g). In addition, the low solubility of octyl silane in water likely decreased its reactivity and led to the lowest GA. The hydrolysis kinetics of propyl and hexyl silanes has not been investigated so far. Presumably, BGC-hexyl undergoes fast hydrolysis under acidic conditions, favoring the final condensation onto the cellulose surface.

Bifunctionalized CNCs from aqueous silylation of CNCs with amino and alkyl silanes

The bifunctionalized CNCs were synthesized using both amino and alkyl (propyl- and hexyl-) silanes in alkaline conditions. Especially, a one-pot reaction in which both amino and alkyl silane agents were added simultaneously was compared with the sequential two-step reactions. Based on nitrogen and silicon contents, Fig. 8 presents that the one-pot reaction (BGC-mix 9) led to a higher GA. This finding may be explained by a synergistic co-reaction of both silane reagents due to a decreased electrostatic repulsion acting between the amine moieties in the presence of uncharged propyl silanes.

The modification of BGC-mix 10 and BGC-mix 11 using two-step sequential reactions, i.e., the addition of amino silane followed by propyl alkyl silane or vice versa, respectively, led to lower nitrogen and silicon concentrations, suggesting that the sequential condensation reaction was affected by the previously formed Si–O-cellulose bonds. Consequently, BGC-mix 12 (with amino and hexyl silanes) was synthesized following a one-pot reaction by incorporating APTES simultaneously with a hexyl silane (HTS). The BGC-12 possessed high GA, but lower nitrogen and silicon concentrations compared to BGC-mix 9, alluding to a lower reactivity when the alkyl chain length increased, as seen in Fig. 8.

Hydrophobicity of silylated CNC films

The hydrophobicity of the pristine and silane grafted cellulose surfaces was evaluated by measuring the static and dynamic contact angles on CNC films. The silylation reactions increased the contact angles of all the films, particularly when an alkyl chain was grafted

Table 4 Static and dynamic contact angles of pristine and silylated BGC cellulose nanocrystals films

Sample	Contact angle (°)			
	Static	Advancing	Receding	Hysteresis
BGC	51 ± 3	53 ± 3	27 ± 3	26 ± 4
BGC-ami 7	89 ± 5	75 ± 4	40 ± 2	35 ± 3
BGC-mix 9	135 ± 4	137 ± 2	108 ± 3	29 ± 7
BGC-mix 10	100 ± 3	96 ± 1	62 ± 2	34 ± 2
BGC-mix 11	101 ± 3	95 ± 2	62 ± 2	33 ± 2
BGC-mix 12	117 ± 3	106 ± 4	72 ± 3	34 ± 5

on the CNC surface, as summarized in Table 4. The highest contact angle value (135°) was recorded with BGC-mix 9 obtained from the one-pot bifunctionalization reaction, proving that the dual grafted CNCs were converted to strongly hydrophobic. The contact angle values also correlated with the GA(nitrogen and silicon content) of the films. In addition, the length of the alkyl chain influenced the final hydrophobicity of the CNC films. For example, BGC-mix 12 had a significantly lower content of alkyl silanes compared to BGC-mix 9 (Fig. 8), but the presence of longer alkyl chains (hexyl vs. propyl) resulted in a relatively high contact angle of 117° (vs. 135°). The hysteresis of ARCAs was higher for the functionalized BGC CNC samples compared to the pristine BGC CNC sample. This is probably related to a further increase in the chemical inhomogeneity and the roughness of the surface of functionalized CNC films. Nevertheless, the contact angle results indicated a strong hydrophobization of the grafted CNC films, which is a crucial parameter for evaluating CNC performance as flotation collectors. Images of sessile drops on film surfaces are presented in Fig. S4.

Zeta potential of silylated CNCs

The previous work by Hartmann et al. (Hartmann et al. 2018) showed that positively charged aminated CNCs could be properly physisorbed on negatively charged quartz and withstood desorption under turbulent flotation regimes (Hartmann et al. 2021), alluding to the importance of both surface charge and hydrophobicity in interactions of CNCs and mineral surfaces. Most of the silylated CNCs functionalized in the present study also displayed a positive ζ-potential under acidic conditions, as shown in Fig. 9. The CNCs

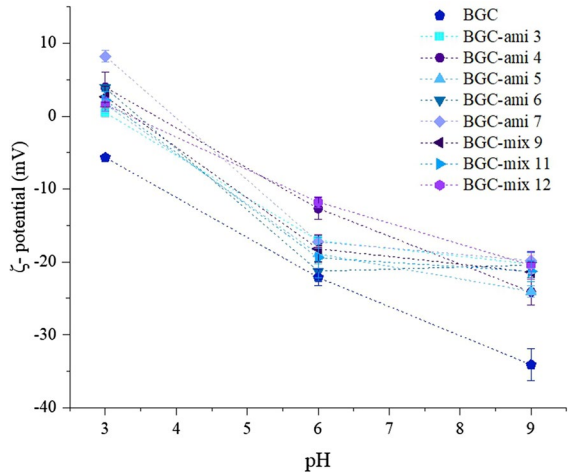

Fig. 9 ζ- potentials of pristine and silylated BGC cellulose nanocrystals (CNCs) grafted with amino silane (BGC-ami) and bifunctionalized CNCs with alkyl and amino silanes; error bars represent standard deviations

with negative ζ-potential, throughout the examined pH range, are presented in Fig. S2. The ζ-potential was dependent on the grafting amount, i.e., a more positive ζ-potential was obtained for samples with a higher amino content (Fig. 6). For instance, at a pH of 3, BGC-ami 4 showed a ζ-potential of 3.9 mV, while BGC-ami 1, BGC-ami 2, and BGC-ami 8 had a negative ζ-potential of − 5.2, − 6.5, and − 5.4 mV, respectively, which correlates with the GA values. In contrast, although a higher amino content was measured for BGC-ami 4 and BGC-mix 9 compared to BGC-ami 7, the highest ζ-potential was obtained with BGC-ami 7 (8.2 mV). This phenomenon shows that the ζ-potential was also affected by other parameters such as the orientation and distribution of the functional groups on the cellulose surface. In addition, the presence of alkyl chains on the cellulose surface did not significantly influence the ζ-potential, as can be seen by comparing BGC-ami 7 with BGCs-alkyl (-propyl, -hexyl, -octyl) at a pH of 3, showing a ζ-potential of − 5.2, − 4.0, and − 4.4 mV, respectively. Overall, the alkyl-containing BGC CNC samples showed similar ζ-potentials as the pristine BGC CNC (− 5.7 mV), supporting that the ζ-potential was only marginally changed due to the presence of an alkyl chain on the CNC surfaces. Interestingly, the results showed that all the samples having a GA of above 0.9 mmol/g were positively charged at a pH of

3. The functionalized samples containing a low content of nitrogen, i.e., lower than 0.9 mmol/g, showed an electric potential around 0 mV. At pH values of 6 and 9, all the pristine and functionalized CNC samples had a negative ζ-potential. The isoelectric point (IEP) for BGC-ami 3, 4, 5, 6, 7, and DES-ami 5 and BGC-mix 10, was between pH values of 3 and 4. For the BGC-alkyl samples, the IEP was not found within the examined pH range.

The performance of silylated CNCs as a flotation agent in quartz microflotation

For the microflotation experiments, three CNC samples were selected and tested as flotation agents for quartz. The samples used were BGC-ami 7, BGC-mix 9, and BGC-mix 12 based on their positive ζ-potential at a pH of 3 and degree of hydrophobicity (TEM images are shown in Fig. S5). The experiments were performed at a pH of 3, at which the CNCs possessed positive ζ-potentials, while quartz particles were slightly negatively charged (see Fig. S6), and attractive electrostatic interactions were assumed to occur. The flotation recovery of quartz particles using CNCs as an additive is shown in Fig. 10. The general recovery was below 15%, indicating a low efficiency of the functionalized BGCs samples. The poor performance may be due to the low ζ-potential difference between CNCs and quartz at a pH of 3, leading to an insufficient electrostatic attraction of CNCs onto the quartz surface, and thus low adsorption densities or an immediate detachment of quartz particles from bubbles during flotation tests. Furthermore, the detected high contact angles indicate that the CNC samples were strongly hydrophobic, which could lead to poor dispersion of the CNC samples in water, and thus a practical absence of CNCs in the flotation slurry.

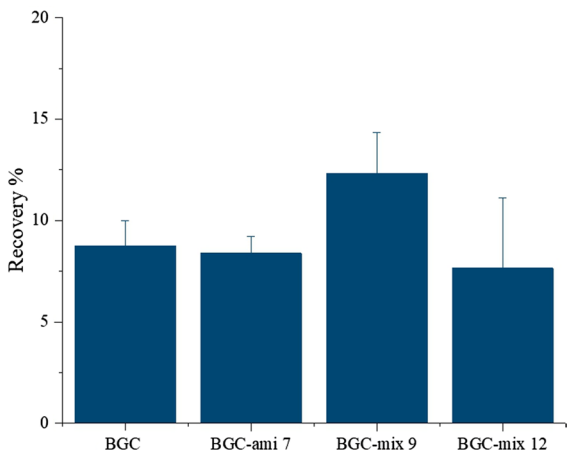

Fig. 10 Quartz recovery in microflotation using silylated CNCs as an additive

Conclusion and outlook

Aqueous one- and two-step silylation routes were considered to functionalize cellulose nanocrystals with different silanes, i.e., an amino silane, alkyl silanes, and mixed structures containing both amino and alkyl silane chains. Primarily, this research aimed to obtain a novel type of bifunctionalized, mixed CNCs that contained both positively charged surface moieties and alkyl chains to enhance the hydrophobic character of the nanoparticles. When the reaction was performed at a pH of 10 compared to pH 4, and when the mass ratio between cellulose and the silane reagent increased, the GA of amino silylation increased. The bifunctionalization conducted by simultaneously adding an amino silane and alkyl silane led to a higher GA than sequential reactions with individual reagents. The hydrophobicity of the CNCs was strongly altered after the functionalization, leading to water contact angles of up to 135° on CNC films, while the silylation only slightly altered the ζ-potential of the functionalized CNCs with amino silanes. The positive ζ-potential is a prerequisite for the successful performance of amino-containing nanocelluloses as flotation reagents and affects the interaction and orthokinetic attachment of nanocelluloses onto quartz surfaces. Consequently, the performance of selected CNCs in quartz flotation was poor due to an insufficient electrostatic attraction between CNCs and quartz particles. Future studies will be devoted to optimizing the functionalization, targeting higher amino contents to increase the positive ζ-potential of CNCs and allowing for sufficient adsorption of modified CNCs on quartz. Further, the effect of the degree of hydrophobicity on the dispersion of CNCs in the flotation slurry has to be tested in the future, as well as the attachment of CNC-coated quartz particles to air bubbles.

Acknowledgments The research leading to these results received funding from the Horizon 2020 Program of the

European Community under Grant Agreement no. 812580 (MSCA-ETN SULTAN) and Academy of Finland project "ACNF" (325276). R.H would like to thank the Academy of Finland for their financial support with the "BioMInt" (13324592) Postdoctoral Research Project. This research benefited from the RAMI- RawMatTERS Finland Infrastructure. In addition, we would like to thank Dr. Martin Rudolph and his group of the Helmholtz Institute Freiberg for Resource Technology for the opportunity to use the OCA 50 (DataPhysics, Germany).

Author contributions All authors contributed to the study conception and design. Material preparation, data collection and analysis were performed by F. L., the zeta potential measurements were performed by R. H. The first draft of the manuscript was written by F. L. and all authors commented on previous versions of the manuscript. All authors read and approved the final manuscript.

Funding Open Access funding provided by University of Oulu including Oulu University Hospital. The research leading to these results received funding from the Horizon 2020 Program of the European Community under Grant Agreement no. 812580 (MSCA-ETN SULTAN) and Academy of Finland project "ACNF" (325276). R.H would like to thank the Academy of Finland for their financial support with the "BioMInt" (13324592) Postdoctoral Research Project. This research benefited from the RAMI- RawMatTERS Finland Infrastructure.

Availability of data and materials Not applicable.

Declarations

Competing interests The authors declare no conflict of interests.

Ethics approval and consent to participate The authors declared no potential conflict of interest with respect to the research, authorship, and/or publication of this article.

Consent for publication All authors read and approved the final manuscript.

References

Abdelmouleh M, Boufi S, ben Salah, A., Belgacem, M.N., Gandini, A., (2002) Interaction of silane coupling agents with cellulose. Langmuir 18:3203–3208. https://doi.org/10.1021/la011657g

Abdelmouleh M, Boufi S, Belgacem MN, Duarte AP, Ben Salah A, Gandini A (2004) Modification of cellulosic fibres with functionalised silanes: development of surface properties. Int J Adhes Adhes 24:43–54. https://doi.org/10.1016/S0143-7496(03)00099-X

Andresen M, Johansson L-S, Tanem BS, Stenius P (2006) Properties and characterization of hydrophobized microfibrillated cellulose. Cellulose 13:665–677. https://doi.org/10.1007/s10570-006-9072-1

Beaumont M, Bacher M, Opietnik M, Gindl-Altmutter W, Potthast A, Rosenau T (2018) A general aqueous silanization protocol to introduce vinyl, mercapto or azido functionalities onto cellulose fibers and nanocelluloses. Molecules 23:1427. https://doi.org/10.3390/molecules23061427

Bel-Hassen R, Boufi S, Salon M-CB, Abdelmouleh M, Belgacem MN (2008) Adsorption of silane onto cellulose fibers. II. The effect of pH on silane hydrolysis, condensation, and adsorption behavior. J Appl Polym Sci 108:1958–1968. https://doi.org/10.1002/app.27488

Braga C, de Carvalho AL, Ludovici F, Goldmann D, Silva AC, Liimatainen H (2021) Silylated thiol-containing cellulose nanofibers as a bio-based flocculation agent for ultrafine mineral particles of chalcopyrite and pyrite. J Sustain Metall 7:1506–1522. https://doi.org/10.1007/s40831-021-00439-y

Brochier Salon M-C, Belgacem MN (2010) Competition between hydrolysis and condensation reactions of trialkoxysilanes, as a function of the amount of water and the nature of the organic group. Colloids Surf, A 366:147–154. https://doi.org/10.1016/j.colsurfa.2010.06.002

Brochier Salon M-C, Belgacem MN (2011) Hydrolysis-condensation kinetics of different silane coupling agents. Phosphorus Sulfur Silicon Relat Elem 186:240–254. https://doi.org/10.1080/10426507.2010.494644

Brochier Salon M-C, Abdelmouleh M, Boufi S, Belgacem MN, Gandini A (2005) Silane adsorption onto cellulose fibers: hydrolysis and condensation reactions. J Colloid Interface Sci 289:249–261. https://doi.org/10.1016/j.jcis.2005.03.070

Brochier Salon M-C, Bayle P-A, Abdelmouleh M, Boufi S, Belgacem MN (2008) Kinetics of hydrolysis and self condensation reactions of silanes by NMR spectroscopy. Colloids Surf, A 312:83–91. https://doi.org/10.1016/j.colsurfa.2007.06.028

Daniels MW, Francis LF (1998) Silane adsorption behavior, microstructure, and properties of glycidoxypropyltrimethoxysilane-modified colloidal silica coatings. J Colloid Interface Sci 205:191–200. https://doi.org/10.1006/jcis.1998.5671

Fernandes SCM, Sadocco P, Alonso-Varona A, Palomares T, Eceiza A, Silvestre AJD, Mondragon I, Freire CSR (2013) Bioinspired antimicrobial and biocompatible bacterial cellulose membranes obtained by surface functionalization

with aminoalkyl groups. ACS Appl Mater Interfaces 5:3290–3297. https://doi.org/10.1021/am400338n

Geng B, Wang H, Wu S, Ru J, Tong C, Chen Y, Liu H, Wu S, Liu X (2017) Surface-tailored nanocellulose aerogels with thiol-functional moieties for highly efficient and selective removal of Hg(II) ions from water. ACS Sustain Chem Eng 5:11715–11726. https://doi.org/10.1021/acssuschemeng.7b03188

Goussé C, Chanzy H, Cerrada ML, Fleury E (2004) Surface silylation of cellulose microfibrils: preparation and rheological properties. Polymer 45:1569–1575. https://doi.org/10.1016/j.polymer.2003.12.028

Hartmann R, Kinnunen P, Illikainen M (2018) Cellulose-mineral interactions based on the DLVO theory and their correlation with flotability. Miner Eng 122:44–52. https://doi.org/10.1016/j.mineng.2018.03.023

Hartmann R, Rinne T, Serna-Guerrero R (2021) On the colloidal behavior of cellulose nanocrystals as a hydrophobization reagent for mineral particles. Langmuir 37:2322–2333. https://doi.org/10.1021/acs.langmuir.0c03131

Hettegger H, Beaumont M, Potthast A, Rosenau T (2016) Aqueous modification of nano- and microfibrillar cellulose with a click synthon. Chemsuschem 9:75–79. https://doi.org/10.1002/cssc.201501358

Indarti E, Marwan R, R., Wanrosli, W.D., (2019) Silylation of TEMPO oxidized nanocellulose from oil palm empty fruit bunch by 3-aminopropyltriethoxysilane. Int J Biol Macromol 135:106–112. https://doi.org/10.1016/j.ijbiomac.2019.05.161

Indarti E, Marwan, Wanrosli W D (2020) Effect of temperature on the silylation of nanocrystalline cellulose from oil palm empty fruit bunch with 3-aminopropyltriethoxysilane. IOP Conf Ser: Earth Environ Sci https://doi.org/10.1088/1755-1315/425/1/012065

Jarrah K, Hisaindee S, Al-Sayah MH (2018) Preparation of oil sorbents by solvent-free grafting of cellulose cotton fibers. Cellulose 25:4093–4106. https://doi.org/10.1007/s10570-018-1846-8

Khanjanzadeh H, Behrooz R, Bahramifar N, Gindl-Altmutter W, Bacher M, Edler M, Griesser T (2018) Surface chemical functionalization of cellulose nanocrystals by 3-aminopropyltriethoxysilane. Int J Biol Macromol 106:1288–1296. https://doi.org/10.1016/j.ijbiomac.2017.08.136

Laitinen O, Ojala J, Sirviö JA, Liimatainen H (2017) Sustainable stabilization of oil in water emulsions by cellulose nanocrystals synthesized from deep eutectic solvents. Cellulose 24:1679–1689. https://doi.org/10.1007/s10570-017-1226-9

Osterholtz FD, Pohl ER (1992) Kinetics of the hydrolysis and condensation of organofunctional alkoxysilanes: a review. J Adhes Sci Technol 6:127–149. https://doi.org/10.1163/156856192X00106

Rafieian F, Mousavi M, Yu Q, Jonoobi M (2019) Amine functionalization of microcrystalline cellulose assisted by (3-chloropropyl)triethoxysilane. Int J Biol Macromol 130:280–287. https://doi.org/10.1016/j.ijbiomac.2019.01.108

Saini S, Belgacem MN, Bras J (2017) Effect of variable aminoalkyl chains on chemical grafting of cellulose nanofiber and their antimicrobial activity. Mater Sci Eng, C 75:760–768. https://doi.org/10.1016/j.msec.2017.02.062

Salon M-CB, Gerbaud G, Abdelmouleh M, Bruzzese C, Boufi S, Belgacem MN (2007) Studies of interactions between silane coupling agents and cellulose fibers with liquid and solid-state NMR. Magn Reson Chem 45:473–483. https://doi.org/10.1002/mrc.1994

Sirviö JA, Visanko M, Liimatainen H (2016) Acidic deep eutectic solvents as hydrolytic media for cellulose nanocrystal production. Biomacromol 17:3025–3032. https://doi.org/10.1021/acs.biomac.6b00910

Yu L, Zhang Z, Tang H, Zhou J (2019) Fabrication of hydrophobic cellulosic materials via gas–solid silylation reaction for oil/water separation. Cellulose 26:4021–4037. https://doi.org/10.1007/s10570-019-02355-7

Zhang Z, Sèbe G, Rentsch D, Zimmermann T, Tingaut P (2014) Ultralightweight and flexible silylated nanocellulose sponges for the selective removal of oil from water. Chem Mater 26:2659–2668. https://doi.org/10.1021/cm5004164

Zhang Z, Tingaut P, Rentsch D, Zimmermann T, Sèbe G (2015) Controlled silylation of nanofibrillated cellulose in water: reinforcement of a model polydimethylsiloxane network. Chemsuschem 8:2681–2690. https://doi.org/10.1002/cssc.201500525